A direct approach for high-quality MEMS based IMU/INS production

L. Poletti, D. Sendra Sanchis, R. Siryani

SBG Systems
1 Avenue Eiffel
78420 Carrières-sur-Seine
FRANCE

Inertial Sensors and Systems 2020
Braunschweig, Germany

978-1-7281-6848-7/20/$31.00©2020 IEEE

Abstract

This paper describes an industrial process for microelectromechanical systems (MEMS) based inertial measurement unit (IMU) and inertial navigation systems (INS) production. Producing high accuracy sensor in a limited time and with a robust process is a universal problem in IMU and INS production. The challenge we face today is finding a calibration and a performance validation processes which will systematically get the most of each IMU.

As MEMS based IMU start competing with other technologies based on high-end gyroscopes, the calibration becomes a critical topic to increase the IMU performance. A common technique used on high-end technologies as Fiber-optic Gyroscopes (FOG) is to combine a set of non-specific multi-position observations and a systematic calibration method as a Kalman filter [1-4]. However, this method requires ultra-low-noise gyroscopes with excellent bias stability and repeatability to correctly measure Earth rotation rate. These attributes are hardly found on MEMS. The method also limits the observability of non-linearities and cross-axis sensitivity errors because of low dynamics.

The calibration method proposed here is based on a direct process [5] combined with high dynamics. High dynamics help discarding noise and bias stability from a proper measurement. Also, a direct approach allows to master all the process and gives the possibility to separate and compensate sensors manufacturing and calibration tools imperfections.

Finally, the performance assessment and acceptance test presented in this paper are used to check the consistency of the direct approach technique by applying high dynamics after calibration and measuring sensor errors and triads misalignment in a whole temperature range as shown in Figure 1.

1. Introduction

SBG systems is an IMU and INS manufacturer, which has developed its knowledges in sensor qualification, integration, and calibration for over 13 years. As a MEMS integrator, SBG systems teams take up the challenge of designing and implementing a robust and fully automatized production workflow.

The production process starts with the assembling of raw material to get IMUs. Then, each IMU is calibrated on a temperature controlled double axes rate table. Once the calibration is finished a calibration report is automatically generated for each IMUs and products are

leaved for an aging process. After this process, performance of all IMUs are reevaluated on the double axes rate table during a performance assessment process. This process automatically generates a report which sums-up all IMU residual errors and every validation criterion. If the product passes these criteria it goes through a final acceptance test which consist in validating electrical and functional features of the product. Once, all these steps are passed the product becomes a finished product and a final report is provided for each unit. Every generated report is systematically stored in a data base which allows us to follow the accuracy of sensors, production tools, algorithms and global IMU performance.

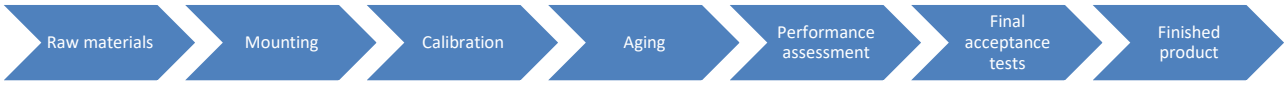

Figure 1. Production workflow

This paper first focuses on the calibration part. Then, it describes production methods to assess sensors performance after calibration. Last, it presents results after calibration.

2. Calibration

Calibration is one of the most critical topics in IMU and INS production workflow. This process increases significantly IMU accuracy and consequently INS accuracy. To get the most of an IMU by calibration it is needed to establish both a precise measurement model of the product and a mechanical tolerance model of the calibration tool. Then, from those models it is possible to suggest an ideal calibration protocol.

2.1. Measurement model

IMU measurement model can be split into two main categories: sensor measurement model which regroup every intrinsic sensors errors and triad measurement model which regroups errors related to clusters of several sensors.

Sensor measurement model can also be divided into two sub-categories deterministic errors and non-deterministic errors.

Non-deterministic errors cannot be calibrated because of its unpredictable behavior. Notwithstanding, those errors can be quantified thanks to an Allan variance analysis [6] (see Figure 2.).

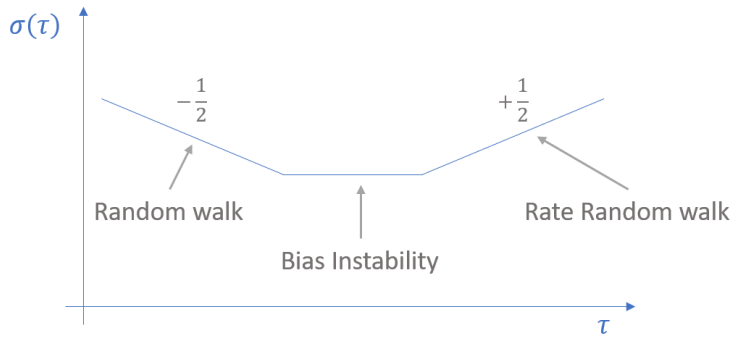

Figure 2. Schematic representation of an Allan variance plot

The first error is due to white noise. It can be measured by fitting the $-1/2$ slope in the first part of the Allan variance plot [7]. For gyroscopes, the white noise is quantified in terms of its power spectral density in $\frac{deg}{s.\sqrt{Hz}}$ or $\frac{deg}{hour.\sqrt{Hz}}$ units and for accelerometers, in terms of $\frac{g}{\sqrt{Hz}}$ or $\frac{m}{s^2.\sqrt{Hz}}$. When the white noise is integrated over time to obtain angular orientation or velocity, it becomes a random walk which is called Angle Random Walk (ARW) and expressed in deg/√hour units for gyroscopes or Velocity Random Walk (VRW) expressed in m/s/√hour for accelerometers. The white noise is a random signal with a constant power spectral density, and it can be averaged to attenuate its impacts on calibration.

The second error is called bias instability. This is a non-deterministic effect that can be modeled using flicker noise. It is also a random process and it can be distinguished from a white noise by a lower frequency spectrum. As this noise is very significant at low frequencies, removal by averaging samples can be particularly troublesome. Because of that, it is often referred to as the true resolution of the sensor. Allan Variance analysis is usually used to quantify the bias instability by taking the lowest value of the flat profile of the curve.

On the contrary, deterministic sensors errors can be calibrated because of its nature. These regroup biases, scale factor errors, non-linear behavior along measuring rang and specifically for gyroscopes acceleration sensitivity.

$$\tilde{f_a} = \mu_a . k_a . (f_a + w_a) + b_a \quad (1)$$

$$\tilde{f_g} = \mu_g . k_g . (f_g + w_g) + b_g + G(A) \quad (2)$$

Equations 1 and 2 define the measurement model of accelerometers and gyroscopes considering all the deterministic errors. Where the bias $b_.$ is defined as an offset occurring

regardless of sensor input. The Scale factor $k_.$ is defined as a gain proportional to sensor input. The Non-linear behavior $\mu_.$ is defined as gain function of sensor input. The gyroscope acceleration sensitivity G is defined as an offset error which occurs when gyroscopes undergo acceleration A.

Note: a, g, and s subscript refer to respectively accelerometer, gyroscope, and sensor in the entire paper.

Every previous error is intrinsic to each sensor. It is also important to consider errors related to a sensor triad. This group of errors is only composed of deterministic effects so they can be calibrated and all of them are consequences of design and manufacturing constraints.

The first triad related error is called cross-axis and it affects accelerometer as well as gyroscope triads. It is defined as a non-exact orthogonality between sensors of the same kind. It is represented by a misalignment matrix M_s (see Equation 4).

$$\widetilde{F_s} = M_s . F_s \tag{3}$$

$$M_s = \begin{bmatrix} m_{xx} & m_{xy} & m_{xz} \\ m_{yx} & m_{yy} & m_{yz} \\ m_{zx} & m_{zy} & m_{zz} \end{bmatrix} \tag{4}$$

Where m_{xx} refers to the measurement obtained on x sensor when applying a stimulation along x axis, m_{xy} refers to the measurement obtained on x sensor when applying a stimulus along y axis, and so on.

The second triad related error is called size-effect and it only affects accelerometers. It is defined as a residual acceleration which occurs under rotation when accelerometer centers of measurement are not coincident. Due to obvious physical constraint it is impossible to make high-end single axis accelerometers point of measurement coincident (see Figure 3). These distances from an ideal center of measurement will generate centripetal and tangential acceleration which must be cancelled. The error equations 5 and 6 are easily obtained from deriving mechanical equation of movement [4].

$$\tilde{F} = M . (F + S(\Omega)) \tag{5}$$

$$S(\Omega) = \overbrace{\begin{bmatrix} r_{xz}.\omega_x\omega_z - r_{xx}.\left(\omega_z^2 + \omega_y^2\right) + r_{xy}.\omega_x.\omega_y \\ r_{yz}.\omega_y\omega_x - r_{yy}.(\omega_x^2 + \omega_z^2) + r_{yz}.\omega_y.\omega_z \\ r_{zy}.\omega_z\omega_y - r_{zz}.\left(\omega_y^2 + \omega_x^2\right) + r_{zx}.\omega_z.\omega_x \end{bmatrix}}^{Centripetal} + \overbrace{\begin{bmatrix} r_{xy}.\dot{\omega}_z - r_{xz}.\dot{\omega}_y \\ r_{yz}.\dot{\omega}_x - r_{yx}.\dot{\omega}_z \\ r_{zx}.\dot{\omega}_y - r_{zy}.\dot{\omega}_x \end{bmatrix}}^{Tangential} \quad (6)$$

Where $r_{..}$ denotes distance between sensor center of measurement $C_{.}$ and triad ideal center along C_s, $\omega_{.}$ denotes rotations around subscripted axis and Ω is the global rotation.

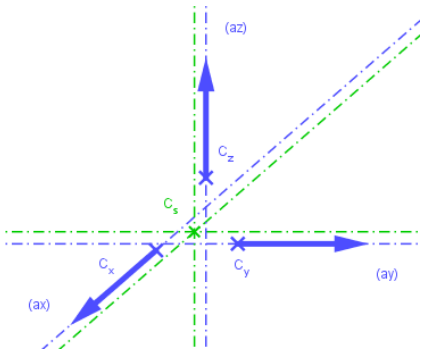

Figure 3. Size effect representation for accelerometer Z axis.

The last triad related error is referred to as triads misalignment. It is defined as a rotation matrix $R_{:}$ between two theoretically parallel sensors triad as shown in Equation 7.

$$\begin{bmatrix} X_g \\ Y_g \\ Z_g \end{bmatrix} = R_a^g.\begin{bmatrix} X_a \\ Y_a \\ Z_a \end{bmatrix} \quad (7)$$

Where g and a subscript respectively refer to gyroscope and accelerometer.

Finally, it is to be noted that every single error listed above depend on temperature. Figure 4 presents an example of accelerometers bias drift correlated to temperature variation. Calibration becomes crucial as the temperature-induced drift on bias, scale factor, non-linearities and cross-axis errors limits the MEMS potential applications in real-world missions [8].

Moreover, thermal hysteresis is also present on MEMS as the Z accelerometer shows in Figure 4. This kind of drift has a non-linear dependance on temperature as it possesses memory and direction dependance [9].

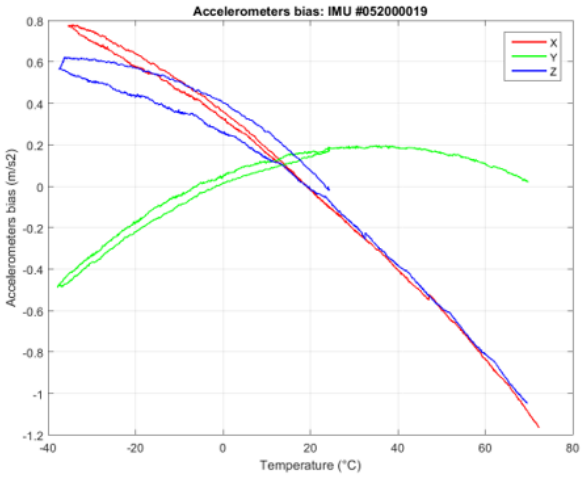

Figure 4. Temperature dependence.

2.2. Calibration tool error model

Calibrations are usually done thanks to specific tools such as Granite calibration surface plate, single, double, or even triple axis rate tables. A double axes rate table has been chosen here for several reasons. Firstly, a granite calibration surface plate is not appropriate neither for high quality nor for mass production. In fact, the calibration process handle by a technician is necessary less repeatable than done by a machine. Secondly, a single axis rate table implies several mounting and demounting operations which is also not appropriate for mass production and which could reduce calibration accuracy because of mechanical tolerances and repeatability. Thirdly, a double axes rate table has enough degrees of freedom to stimulate sensors in every direction with only one mounting operation, consequently it is not needed to have further degrees of freedom. In this sense, a triple axes calibration rate table is over determined. This means that a given stimulation can be applied by more than one set of calibration tool inputs. Then, this unnecessarily increases the complexity of mechanical tolerance and consequently the risk of uncontrolled defects.

In fact, it is important to establish an error model of the double axes rate table for a better understanding of tools tolerances influence on IMU calibration. To do so, every mechanical part of the double axis rate table has been associated to a frame or axis. Firstly, we define the Earth frame (E). This frame is associated to the earth, X_E and Y_E axes belong in equator plan and X_E axis cross the prime meridian as described in [10]. Secondly, we define the Navigation frame (N). This frame is associated to the local cardinal points X_N, Y_N and Z_N are respectively aligned to North, East and Down as shown in Figure 5.

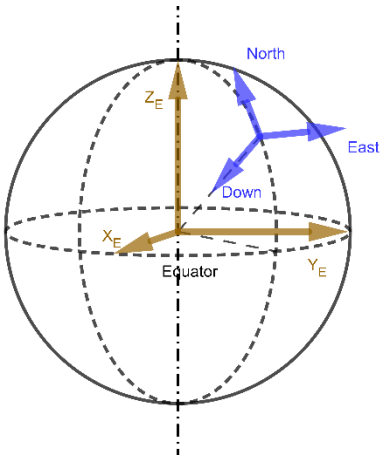

Figure 5. Earth related frames.

Thirdly, we define the Outer axis (o) and the Inner axis (i). The Outer axis corresponds to the horizontal axis of the rate table which control the first gimbal. It is aligned by design to East-West axis. The Inner axis corresponds to the vertical axis of the rate table which controls the second gimbal. Fourthly, we define the Table frame (T) which is associated to the plate (or second gimbal) on which IMU are mounted. Fifthly, we define the Body frame (B), which is the theoretical IMU frame. And lastly, we define the Sensors frame (S), which is associated to each sensor triad.

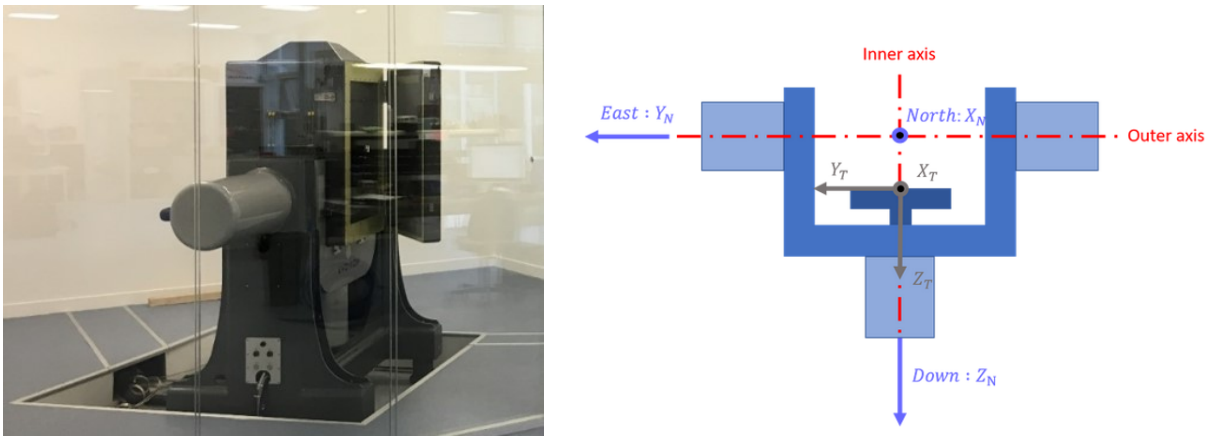

Figure 6. Picture of (left) a double axes rate table and (right) its associated frames and axes.

Each coupled of frames are linked by a rotation that characterizes either a mechanical degree or a mechanical tolerance:

- R_E^N characterizes rotation rate observation depending on latitude.
- R_N^o refers to the outer axis initial orientation and horizontal defect and East-West misalignment.

- R_i^o characterizes Outer and Inner axis orthogonality defects, Inner axis initial orientation imperfection and Up-down misalignment.

- R_i^T, R_T^B and R_B^S can be regrouped into one rotation R_i^S as all mechanical parts are assumed to be rigidly attached.

The scheme in Figure 7 sums up every frames and rotation from Earth frame to Sensor frame.

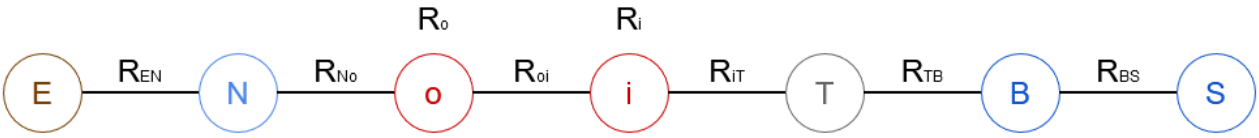

Figure 7. Frames chain.

This frame chain gives us enough information to model the gravity and earth rotation rate observation for a given set of mechanical tolerances and a given set of axes inputs.

$$\overrightarrow{f_a}(\theta_o, \theta_i) = R_i^A . R_i(\theta_i) . R_o^i . R_o(\theta_o) . R_N^o . \overrightarrow{g_N} \tag{8}$$

$$\overrightarrow{f_g}(\theta_o, \theta_i) = R_i^G . R_i(\theta_i) . R_o^i . R_o(\theta_o) . R_N^o . R_E^N . \overrightarrow{\Omega_E} \tag{9}$$

As shown in Equations 8 and 9, θ_i and θ_o respectively refer to calibration tool orientation input around inner and outer axes.

2.3. Direct approach

Sensor calibration direct approach consists in estimating each parameter one by one in a specific order to attenuate the correlation between different errors. The main steps of this process is the non-deterministic error attenuation, sensors calibration and triads calibration.

Noise is attenuated by averaging measurements over a duration (τ) determined for each sensor through an Allan variance analysis [6]. This duration must respect two criteria: it must be long enough to get the most precise measurement and it must be short enough to do not undergo bias instability and rate ramp effects. This value can be observed on an Allan variance plot as the intersection of random walk slope and bias instability value as shown in Figure 8.

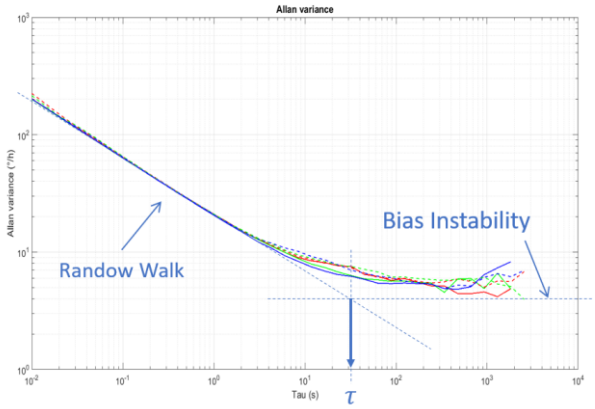

Figure 8. τ determination using Allan variance plot

Sensor calibration begins with getting rid of the bias b_s. The basic idea to estimate the bias is to compute the average value of two opposite measurements (see Equation 10). This is supposed to get rid of external input such as gravity or earth rotation rate.

$$\widehat{b_s} = \frac{1}{2}.\left[\widetilde{f_s^+} + \widetilde{f_s^-}\right] \tag{10}$$

Where $\widetilde{f_s}$ refers to a given sensor measurement and superscript + and - indicate if the associated stimulation is positive or negative.

It has been proven that the most precise way to estimate accelerometer bias is to select measurement along horizontal plan as those are slightly impact by scale factor and gyroscopes bias can also be directly observed through static measurements taken orthogonally to earth rotation rate.

For following parameters estimations, earth rotation rate observations must be considered. There are at least two solutions to cancel earth rotation rate: by post processing orientation and manually subtract it from each measurement, or by carrying out measurements under specific conditions of orientation to compensate earth rotation rate.

The scale factor k_s is estimated by stimulating each sensor with two opposite inputs. Thus, it is possible to cancel the bias by subtracting measurement couple as shown in Equation 11. Generally, gravity is used as accelerometer input and gyroscopes are stimulated by a specific rotation rate around axis.

$$\widehat{k_s} = \frac{1}{2.f_{sti}}.\left(\widetilde{f_s^+} - \widetilde{f_s^-}\right) \tag{11}$$

Where f_{sti} refers to the stimulus applied to the sensor.

For non-linearities μ_s the same process for Scale Factor is extended to the full sensor measurement range. Therefore, sensor is stimulated with positive and negatives inputs along its whole range.

$$\widehat{\mu_s(f_{sti})} = \frac{\tilde{f}_s - \hat{b}_s}{f_{sti}} \tag{12}$$

The resulting data set is stored to be used by interpolation during real time acquisition.

Considering triads effects, cross-axis errors are estimated by applying a set of opposite stimulations on sensors along three dimensions. This will make appear residual projection of stimulations on each axis. As for scale factor estimation, bias effect is cancelled by subtracting each couple of opposite measurements. And generally, gravity is used as accelerometer input and gyroscopes are stimulated by a specific rotation rate around axis. From those observation one can compute each misalignment matrix as shown in Equation 13.

$$m_{s_1 s_2} = \frac{1}{2.f_{sti}} . \left(\widetilde{f^{+}_{s_1 s_2}} - \widetilde{f^{-}_{s_1 s_2}} \right) \tag{13}$$

Where $f_{s_1 s_2}$ refers to a measurement obtained on s_1 sensor when applying a stimulation along s_2 axis.

Accelerometer triad to gyroscopes triad alignment is naturally done by fixing orthogonality. However, this alignment is directly impacted by the calibration tool precision. If the verticality error of the table does not belong in a respectable tolerance accelerometers and gyroscopes will be aligned to two significantly different frame as shown in Figure 9.

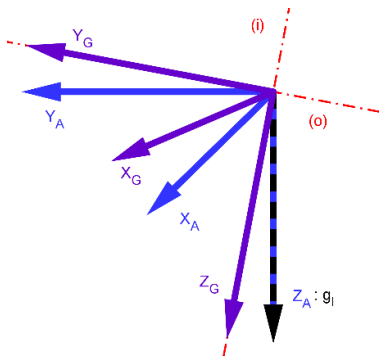

Figure 9, Accelerometer and gyroscope misalignment causes by calibration tool defects.

Concerning accelerometer size effect, distances R_x, R_y and R_z between accelerometers center of measurement from an arbitrary center of IMU are defined by design. From those

definitions it is possible to compensate centripetal part of residual accelerations as shown in Equation 14.

$$S(\Omega) = \overbrace{\begin{bmatrix} r_{xz}.\omega_x\omega_z - r_{xx}.\left(\omega_z^2 + \omega_y^2\right) + r_{xy}.\omega_x.\omega_y \\ r_{yz}.\omega_y\omega_x - r_{yy}.(\omega_x^2 + \omega_z^2) + r_{yz}.\omega_y.\omega_z \\ r_{zy}.\omega_z\omega_y - r_{zz}.\left(\omega_y^2 + \omega_x^2\right) + r_{zx}.\omega_z.\omega_x \end{bmatrix}}^{Centripetal}, R_x = \begin{bmatrix} r_{xx} \\ r_{xy} \\ r_{xz} \end{bmatrix}, R_y = \begin{bmatrix} r_{yx} \\ r_{yy} \\ r_{yz} \end{bmatrix}, R_z = \begin{bmatrix} r_{zx} \\ r_{zy} \\ r_{zz} \end{bmatrix} \quad (14)$$

2.4. Calibration tools specification

Mechanical tolerances of the calibration tool have a huge influence on calibrated IMU accuracy. Table 1 presents the specification key values of the calibration table used to write this article. As mechanical tolerance limits calibration performance, this gives an idea of the minimum precision that can be expected.

Table 1. Double axes rate table key specifications

Parameter	Specification	Units
Inner to outer axis orthogonality	< 1	arcsecond
Wobble	< 5	arcsecond
Inner axis vertical alignment	< 2	arcsecond
Outer axis East-West alignment	< 2	arcsecond

2.5. Calibration results

To prove the consistency of the calibration method a calibration report is automatically generated with the residuals errors for each model computed. To validate the results an IMU embedding three CRH02-200 MEMS gyroscopes was used. This IMU will be referred to further in the text as IMU-SBG-01.

After computing the calibration model, it is theoretically applied to the measured data to guarantee that all the sensors parameters have been fitted with low errors residuals.

Figure 10 presents the bias, scale factor, and non-linearities residuals from the generated report.

ID	Test	Requirement	Axis	Results			Status
				Min	1σ	Max	
1	Sweep bias residuals	≤ 30 °/h	X	-1,370	0,314	1,173	Pass
			Y	-2,042	0,690	1,350	
			Z	-2,422	1,078	2,419	

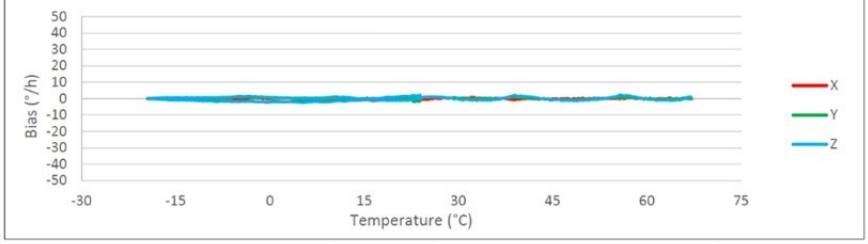

ID	Test	Requirement	Axis	Results			Status
				Min	1σ	Max	
3	Scale Factor residuals	≤ 150 ppm	X	-33,180	19,356	14,465	Pass
			Y	-34,633	24,556	33,890	
			Z	-27,508	17,385	25,052	

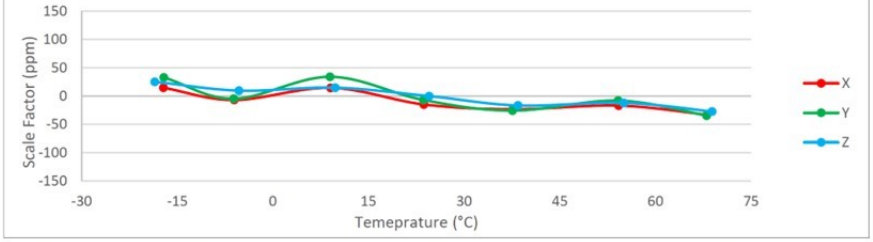

ID	Test	Requirement	Axis	Results			Status
				Min	1σ	Max	
4	Non-linearity residuals	≤ 70 ppm of FS	X	-44,651	23,183	45,833	Pass
			Y	-45,586	22,661	49,522	
			Z	-44,481	21,547	41,809	

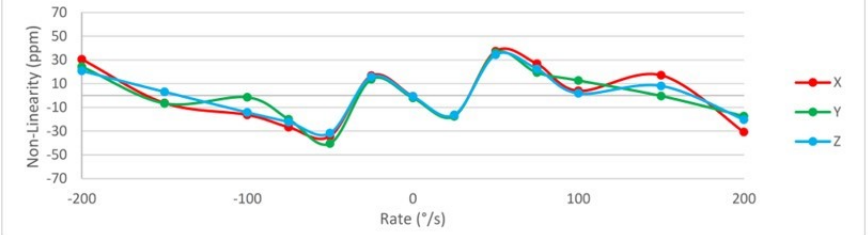

Figure 10. Gyroscopes bias, scale factor and non-linearities residual errors after calibration.

Typical values from the technical datasheet manufacturer of these gyroscopes are taken to be compared to our maximum values in the calibration report in Table 2. The CRH02-200 specifies the following performance on bias, scale factor and non-linearities errors over temperature.

Table 2: Manufacturer datasheet of CRH02-200 compared to calibration results.

Parameter	**Units**	**CRH02-200 specifications (Typical values)**	**IMU-SBG-01 calibration results (Maximum values)**
Bias over temperature	°/h	±3000 Note: with respect to 25°C value	#1 (X): 1.17 #2 (Y): 1.35 #3 (Z): 2.42 Note: Max residuals for all

			temperature range
Scale Factor Variation Over Temperature	ppm	±3000 Note: with respect to 25°C value	#1 (X): 14.46 #2 (Y): 33.89 #3 (Z): 25.05 Note: Max residuals for all temperature range
Scale Factor Non-Linearity	ppm of Full Scale	±200	#1 (X): 45.83 #2 (Y): 49.59 #3 (Z): 41.81 Note: Value et 20°C

It can be observed that after applying the calibration model the intrinsic errors of the sensor can be significantly reduced. For an ideal sensor, with no drift over time, these residuals would be the true performance after calibration. However, it is well known that sensors parameters can drift and present a low repeatability between power cycles and over time. For this reason, to guarantee the best performance it is important to evaluate the IMU accuracy after an aging process. This process depends on the IMU grade and it can last from one day to one month.

3. Validation

After aging the products undergo two validation processes to ensure established specifications. we want to make sure that products are still compliant to established specifications. Then products will undergo two validation process. The first one assesses that sensor errors do not drift over time. The second one is a general electrical and functional check-up.

3.1. Performance assessment

Performance assessments consist in reevaluating every sensor error and quantifying each residue for 3 temperature points.

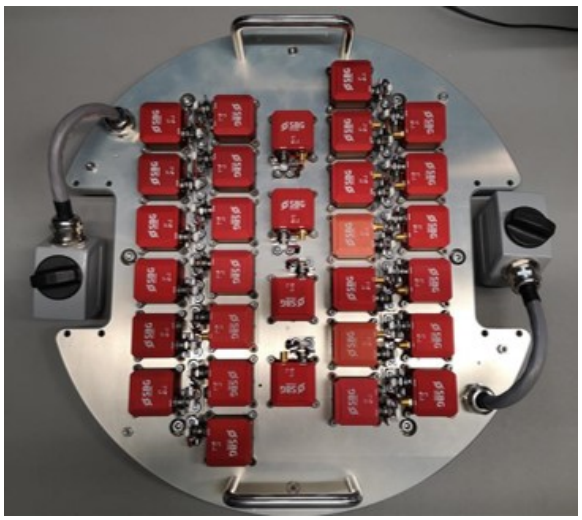

Figure 11. Calibration and performance assessment plate.

First, the warmup bias is assessed. Then, random walk and bias instability are quantified again thanks to an Allan variance study. Residual Start-up bias, Scale factor, nonlinear behaviors and gyroscope acceleration sensitivity are quantified using methods described in calibration part. Results from a gyroscope non-linearities measurement can be observed in Figure 12.

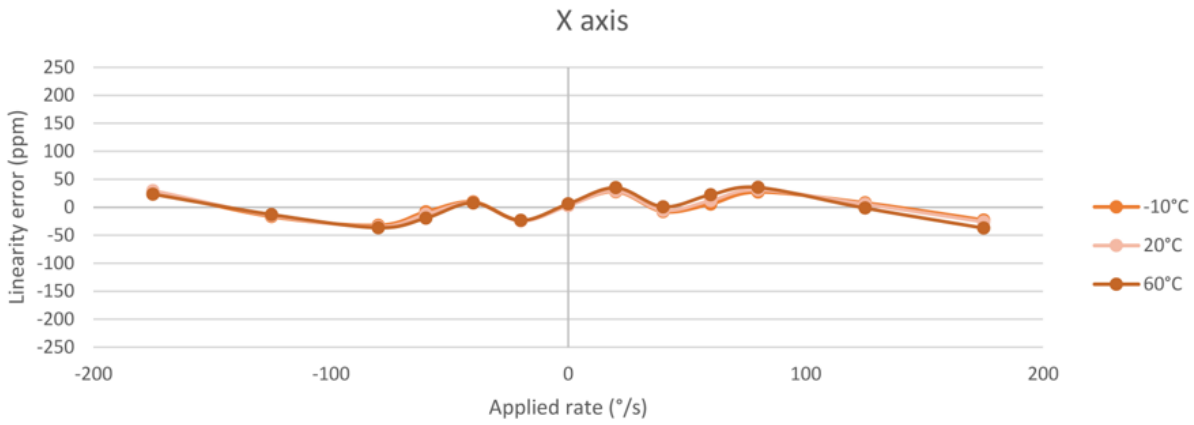

Figure 12. Gyro non-linear residuals

Sensor triad validation is divided into two parts. First, we quantify the orthogonality $\delta_{s_1 s_2}$ as a residual error between a couple of sensors (s_1, s_2) as shown in Equation 15.

$$\delta_{s_1 s_2} = \operatorname{acos}\left(\overrightarrow{M_{s_1}}.\overrightarrow{M_{s_2}}\right) - \frac{\pi}{2} \tag{15}$$

Where M_{s_1} and M_{s_2} refer to reevaluated misalignment matrix lines:

$$M_S = \begin{bmatrix} m_{s_1 s_1} & m_{s_1 s_2} & m_{s_1 s_3} \\ m_{s_2 s_1} & m_{s_2 s_2} & m_{s_2 s_3} \\ m_{s_3 s_1} & m_{s_3 s_2} & m_{s_3 s_3} \end{bmatrix} \begin{matrix} = M_{s_1} \\ = M_{s_2} \\ = M_{s_3} \end{matrix} \quad (16)$$

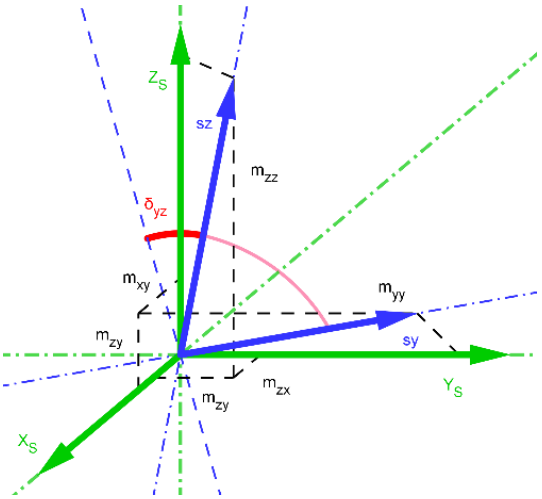

Figure 13. Orthogonality defect residue representation.

Then, misalignment is quantified as a residual rotation relative to the reference surface of the IMU.

To do so, we estimate the rotation matrix R that minimize the error between the misalignment matrix M and a given ideally orthogonal triad (X, Y, Z). This consist in finding the orthogonal matrix R with determinant +1 that minimizes the loss function:

$$L(R) \equiv \begin{cases} X - M_x . R \\ Y - M_y . R \\ Z - M_z . R \end{cases} \quad (17)$$

Where M_x, M_y and M_z refer to reevaluated misalignment matrix lines:

$$M = \begin{bmatrix} m_{xx} & m_{xy} & m_{xz} \\ m_{yx} & m_{yy} & m_{yz} \\ m_{zx} & m_{zy} & m_{zz} \end{bmatrix} \begin{matrix} = M_x \\ = M_y \\ = M_z \end{matrix} \quad (18)$$

This process allows detection of defects during production process and ensures the best product quality.

4.2 Final acceptance tests

To guarantee high quality products, once IMUs have passed performance assessment, a series of electrical and function tests are done.

Those automatized tests aim to control power consumption, sync out frequency, Inputs/Outputs (CAN bus, serial Comm.) and sensors measurement consistency as: ground acceleration, earth rotation rate, magnetic field, temperature, atmospheric pressure consistency. For IMU with high demanding applications ground continuity and insulation tests are done.

In addition of IMU, for INS other functionalities are systematically tested: GNSS constellations, GNSS position, (latitude, longitude, altitude) in a known location, GNSS attitude (Heading, Pitch) for double antenna products.

If the IMU/INS passes every tests it can be stored as a finished product. At the same time, a final report is automatically generated, and all data produced during the entire production process is stored in a data base. This allows the monitoring of performance, and early detection of drifts on sensors parameters or manufacturing process. By plotting histograms IMU specifications are easily defined.

4. Results

Results have been evaluated on IMU-SBG-01. This IMU is composed of three CRH02-200 gyroscopes and three high-end accelerometers. The following study focuses on gyroscopes as they present the major challenge on MEMS high-end applications. Results have been obtained by applying the whole production process on IMU-SBG-01: mounting, calibrating, one week of aging and performance assessing.

An extract of the validation report is presented in Figure 14. It shows composite error measurement from the IMU one week after calibration.

ID	Test	Requirement	Axis	Results			Status
				T_1 (-10°C)	T_2 (20°C)	T_3 (60°C)	
1	Overall bias	≤ 20°/h	X	2,36	1,18	0,88	Pass
			Y	0,49	0,85	0,44	
			Z	-1,78	1,59	-0,15	
5	Scale Factor Error	≤ 250 ppm	X	71,28	75,14	62,90	Pass
			Y	84,90	109,95	107,32	
			Z	65,44	64,80	64,46	
6	Non-linearity Error	≤ 50 ppm RMS of Full Scale	X	19,38	28,56	17,93	Pass
			Y	16,79	25,78	23,86	
			Z	15,84	25,86	19,70	

Figure 14. Overall gyroscopes bias, scale factor and non-linearities error after one week of aging.

Again, these results can be compared to the gyroscopes technical specifications from manufacturer as shown in Table **3**.

Table 3. Manufacturer datasheet of CRH02-200 compared to performance assessment.

Parameter	Units	CRH02-200 specifications	IMU-SBG-01 performance assessment
Bias over temperature	°/h	±3000 Note: with respect to 25°C value	#1 (X): 2.36 #2 (Y): 0.85 #3 (Z): -1.78 Note: Max value for all three temperatures
Scale Factor Variation Over Temperature	ppm	±3000 Note: with respect to 25°C value	#1 (X): 75.14 #2 (Y): 109.95 #3 (Z): 64.80 Note: Max value for all three temperatures
Scale Factor Non-Linearity	ppm of Full Scale	±200	#1 (X): 28.56 #2 (Y): 25.78 #3 (Z): 25.86 Note: RMS value for all three temperatures

Even if before calibration the CRH02-200 presents great performance for a MEMS gyroscope, it can be observed that the direct calibration method improves the gyroscopes specifications. Bias or non-linearities specifications are divided by 10 and scale factor error is divided by 100. This improvement is crucial for high-end navigation applications and it is the only way to guarantee an INS accuracy, repeatability, and reliability. In this sense, a rigorous screening must be performed during production process to deliver IMUs that meet the specifications defined during IMU/INS qualification.

5. Conclusion

By taking care of sensors selection, capitalizing knowledge in mechanical and electronical design, and enhancing production process over years, SBG systems teams have been able to take the most out of MEMS sensors. This paper focuses on the production workflow which has been implemented in recent years. It shows the importance of establishing a robust and meticulous calibration process and particularly the importance to understand each IMU errors as well as calibration tools errors. It also demonstrates the crucial aspect of validating systematically each product to ensure the best quality. The fully automatized calibration and validation process, presented in this paper, allows SBG

Systems to produce thousands of very high performance IMU and INS every year. The extensive quality checks combined with rigorous qualifications and aging tests are the keys to guarantee IMU specifications from unit to unit, over temperature and over the product lifetime.

References

[1] Z. F. Syed, P. Aggarwal, C. Goodall, X. Niu and N. El-Sheimy. (2007). “A new multi-position calibration method for MEMS inertial navigation systems”. Measurement Science and Technology. 18. 1897. 10.1088/0957-0233/18/7/016.

[2] Shin, E.H. & El-Sheimy, Naser. (2002). “A new calibration method for strapdown inertial navigation systems”. Z. Vermess. 127. 1-10.

[3] F. Olsson, M. Kok, K. Halvorsen, T. Schön. (2016). “Accelerometer calibration using sensor fusion with a gyroscope”. 1-5. 10.1109/SSP.2016.7551836.

[4] P. Gao, K. Li, T. Song and Z. Liu. (2017). “An Accelerometers-Size-Effect Self-Calibration Method for Triaxis Rotational Inertial Navigation System”. IEEE Transactions on Industrial Electronics. PP. 1-1. 10.1109/TIE.2017.2733491.

[5] J. Ferguson (2015). “Calibration of Deterministic IMU Errors”, (). Retrieved from https://commons.erau.edu/pr-honors-coe/2

[6] C. Naranjo. (2008). “Analysis and Modeling of MEMS based Inertial Sensors”.

[7] N. El-Sheimy, H. Hou and X. Niu. (2008). “Analysis and Modeling of Inertial Sensors Using Allan Variance. Instrumentation and Measurement”, IEEE Transactions on. 57. 140 - 149. 10.1109/TIM.2007.908635.

[8] Prikhodko, I.P., Zotov, S.A., Trusov, A., & Shkel, A. (2012). “Thermal Calibration of Silicon MEMS Gyroscopes”. IMAPS international conference and exhibition on device Packaging. Fountain Hills.

[9] Gulmammadov, Farid. (2009). “Analysis, modeling and compensation of bias drift in MEMS inertial sensors”. 591 - 596. 10.1109/RAST.2009.5158260.

[10] J. Farrell (2008), “Aided Navigation: GPS with High Rate Sensors”. New York: McGraw-Hill.